

Pre-design of a target assembly for minor actinides transmutation

T. Kooyman, L. Buiro, B. Valentin, G. Rimpault, F. Delage

► **To cite this version:**

T. Kooyman, L. Buiro, B. Valentin, G. Rimpault, F. Delage. Pre-design of a target assembly for minor actinides transmutation. 14th Exchange Meeting on partitioning and transmutation - Actinide and Fission Product Partitioning and Transmutation, Oct 2016, San Diego, United States. hal-02441960

HAL Id: hal-02441960

<https://hal-cea.archives-ouvertes.fr/hal-02441960>

Submitted on 16 Jan 2020

HAL is a multi-disciplinary open access archive for the deposit and dissemination of scientific research documents, whether they are published or not. The documents may come from teaching and research institutions in France or abroad, or from public or private research centers.

L'archive ouverte pluridisciplinaire **HAL**, est destinée au dépôt et à la diffusion de documents scientifiques de niveau recherche, publiés ou non, émanant des établissements d'enseignement et de recherche français ou étrangers, des laboratoires publics ou privés.

Pre-design of a target assembly for minor actinides transmutation

T.Kooyman, L.Buiron, B.Valentin, G.Rimpault, F. Delage

Abstract :

Minor actinides (MA) transmutation options for critical fast reactors are divided in two different approaches, the homogeneous one in which MA are diluted in the driver fuel and the heterogeneous one in which MA are concentrated in UO₂ based fuel in sub-assemblies located at the periphery of the core. This latter option, named minor actinides bearing blankets has a small impact on core behavior, at the expense of lower transmutation performances due to the lower flux level experienced by the targets.

As such, there is an incentive to maximize the volume fraction of minor actinides loaded in the target assemblies in order to achieve optimal transmutation performances. However, a high MA fraction lead to an increase in gas – especially Helium – production and negatively impacts fuel swelling and pressurization of the fuel pin along with its thermo-mechanical behavior. Consequently, an iterative optimization process must be carried out during the pre-design step of such an assembly to optimize both the neutronic and mechanical performances. Using a conservative approach, we assumed that all produced gases were released in the pin free space. This production was evaluated using depletion calculations and the corresponding pin internal pressure and resistance criterion were computed. Centerline temperature of the hottest pin was also evaluated. Sensitivities to technological constraints considered into the model were also computed.

Several options were evaluated to develop a suitable assembly: smear density decrease, plenum size increase, cladding thickness increase and modification of the minor actinides volume fraction. We found that an optimum existed at 47 % of fuel volume fraction, corresponding to a situation with wider pins, thicker cladding and increased gas expansion plenum height compared to standard fuel assemblies. The associated transmutation performances were in the range of -8.2 kg/TWhe, or a 33 % increase in the minor actinides consumption compared to standard fuel assembly design. A pressure drop model was also implemented and it was verified that the pressure drop remained below the one of a standard fuel assembly. The new assembly design impacts on decay heat and neutron source were also assessed and it was shown that a design margin existed for optimization with regards to these impacts.

Introduction:

In the heterogeneous approach of minor actinides transmutation, the nuclei to be transmuted are concentrated in UO₂ based fuels in sub assemblies located at the periphery of the core. This approach exhibits several advantages. It leads to a physical separation of the regular core operation from the transmutation process and more importantly allows the use of two different fuel cycles. It also only slightly impacts core operations due to the peripheral location of minor actinides in the core. However, this specific location means that the transmutation performances are decreased compared to a case where MA are directly loaded into the core as the flux level in the targets area is lower [1].

The limited impact on core behavior allow for compensation of the loss in performances by increasing the minor actinides mass loaded in the blankets, which counterbalance the lower

efficiency of the heterogeneous approach. However, loading of minor actinides has several adverse potential effects on the fuel pins: decrease of thermal conductivity and margin to melting point, increase in gases production, especially Helium due to alpha decay of short lived isotopes such as ^{242}Cm and a possible increase in swelling. The increase in gases production and release can lead to over-pressurization of the pin and clad rupture. Consequently, the increase in fuel volume fraction in the assembly is limited by pin resistance. Additionally, for a given mass to be loaded, there is an incentive to increase the fuel volume fraction in the assembly in order to decrease the Am content in the fuel and thus limit the specific activity of the fuel.

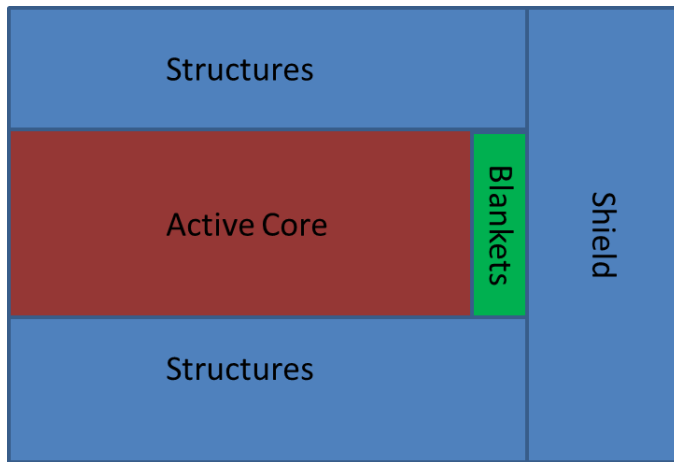
An optimization of the assembly pre-design with regards to the loaded fuel fraction and the pin thermo-mechanical design is carried out here. After presenting the tools and methods used here, an optimal design is presented and commented in terms of assembly behavior and transmutation performances.

1. Tools and methodology

We considered heterogeneous transmutation of minor actinides using uranium oxide as support matrix, as proposed in [2]. The minor actinides isotopic vector used is given in Table 1. It is deemed representative of the vector available in France in 2035. Core calculations were carried using the homogeneous SFR V2b core designed by CEA, EDF and AREVA [3]. Assumptions used on the core management and fuel cycle can be found in [4] and are detailed below. The innermost reflector ring was replaced by target assemblies for minor actinides transmutation, as shown in Figure 1. Neutronic calculations were performed using the ERANOS deterministic code package [5] along with the DARWIN code package for depletion calculations [6]. The JEFF 3.1 nuclear data library [7] with a 33 group energy mesh was used. The analysis of target behavior was carried out at an equilibrium situation in which the transmutation performances are identical over two consecutive cycles. To achieve this equilibrium, it was considered that plutonium produced in the targets was reloaded in the core and minor actinides production of the core loaded in the blankets, which were then topped up to 20 %vol using the initial minor actinides feed.

Table 1 : Isotopic vector used for minor actinides at initial loading

Element	Np237	Am241	Am242m	Am243	Cm242	Cm243	Cm244	Cm245	Cm246
Fraction (%mass)	16.87	60.62	0.24	15.7	0.02	0.07	5.14	1.26	0.08



Dimension	Length (mm)
Inner flat to flat	197.3
Wrapper thickness	4.5
Sodium thickness between assemblies	4.5
Cladding thickness	0.5
Spacing wire thickness	1
Gap	0.15
Plenum height	989
Fissile column height	1000

Figure 1 : 2D-RZ representation of the SFR-V2B core with minor actinides bearing blankets and fuel assembly specifications

Considering the fuel assembly specifications of Figure 2, we can plot the relationship between pin diameter and fuel volume fraction in the assembly, as shown in Figure 1. With regards to the historical data from past SFRs, pin diameters between 5.8 and 15.8 mm were considered, which corresponds respectively to the fuel pins of the FFTF in the USA and of the blanket pins of SuperPhénix in France [8]. The highest achievable fraction is then 55.6 vol% for the assembly parameters of the considered core.

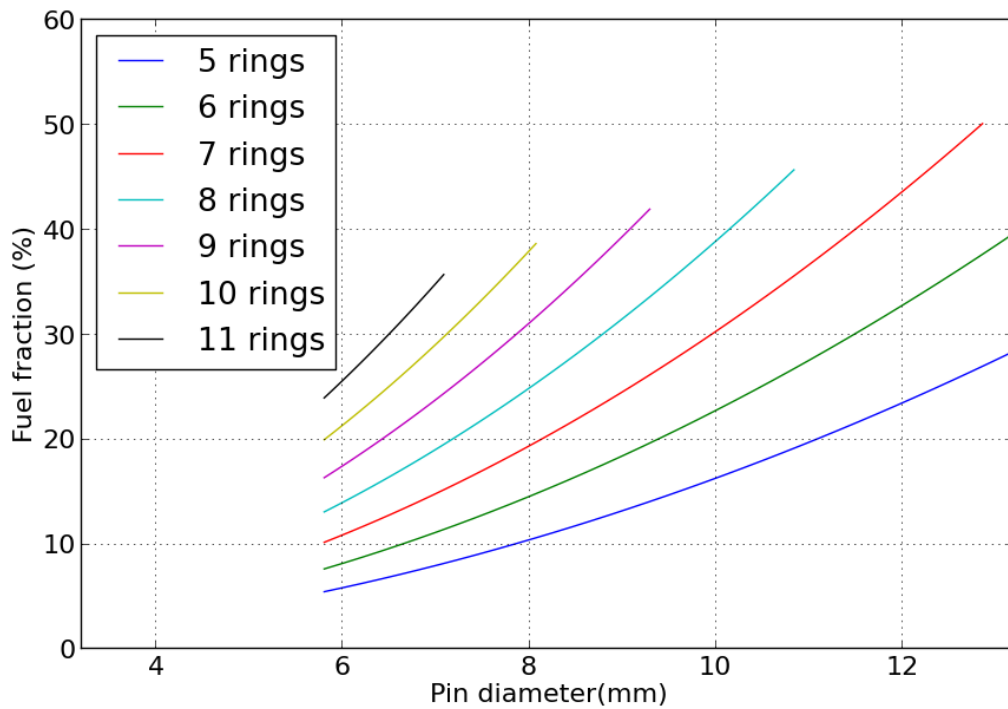


Figure 2 : Fuel fraction vs pin diameter in a SFR V2B assembly

Following what was done in [4], we considered a total irradiation time of 4100 EPFD for a blanket assembly, which is twice the one of a regular fuel assembly. This is done in order to compensate for the low flux level in the periphery of core. At 2050 EPFD, we considered that the assemblies were rotated by 180 °C in order to smooth the irradiation profile in the assembly and thus the gas production profile, as shown in Figure 3. This leads to a reduction of 16 % of the maximal gas production, which decreases the dimensioning constraint by a same margin.

Several parameters must be taken into account during the pre-design phase, namely the cladding resistance, the margin to fuel melting and the assembly pressure drop. All the evaluations were carried out at the end of irradiation when the gas production is maximal and in hot conditions. For neutronic calculations, the radial blanket was divided in nine zones with equal volumes and rotation occurred along the fifth one. The fuel volume fraction was calculated considering a fuel density equal to 88 % of the theoretical density.

Evaluation of the cladding resistance was done using the Von-Mises stress for non-damaged material and thick tube, where the constraint is defined as $P_m = \sqrt{3} \frac{r_{int} r_{ext}}{r_{ext}^2 - r_{int}^2} \Delta p$ with $r_{int,ext}$ the internal and external radius of the clad and Δp the pressure difference on the cladding. The pressure inside the pin was calculated using the DARWIN code system and the conservative hypothesis that all the fission gases and helium produced was released in the free volume of the pin. Pressure level in the pin was evaluated at the end of target irradiation and under hot conditions, which is the most penalizing case. As no solid swelling model for minor actinides fuels is available, solid swelling considerations were not included in this work. The innermost blanket ring was used as it is the dimensioning zone for pin design here. 50 days refueling outages were taken into account to factor in the helium production due to the decay of short-lived isotopes such as ^{242}Cm . Gas temperature

was taken at 428.7 °C. The maximum admissible strain was taken as the one of ODS steel cladding and the strain criterion was defined as the ratio of P_m over this value.

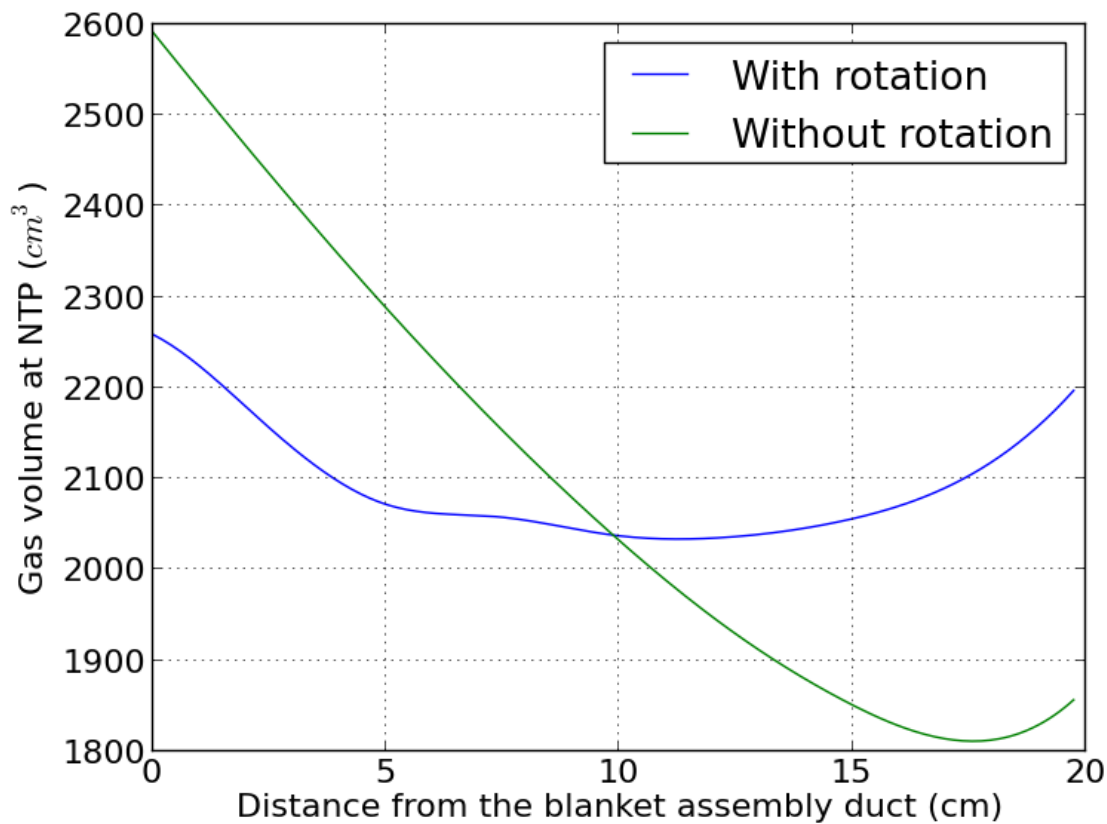


Figure 3 : Effect of rotation on gas production distribution

Fuel centerline temperature was calculated using the relation derived by Nishi in [9] for thermal conductivity of the $UAmO_2$ and defined as $\lambda (W.m^{-1}.K^{-1}) = (0.1006 + 1.664.10^{-4}T(K))^{-1}$ and an inner clad temperature of 620 °C. Gap thermal conductivity was taken as 0.280 $W.m.K^{-1}$, which is the one of pure Helium at 700K taken from [10]. It should be noted that according to [9], the thermal conductivity of a sub-stoichiometric americium oxide is lower than the one of $UAmO_2$. A minimum value of 1 $W.m^{-1}.K^{-1}$ has alternatively been considered in this paper for comparison purpose.

The maximum fuel centerline temperature was taken arbitrarily taken at 1800 °C, considering a maximal peaking factor of 1.26. Looking at Figure 5, the temperature limit is no longer a dimensioning constraint above 1800 °C. However, considering the lower melting temperature for minor actinides dioxides [11], it may be necessary to lower this limit depending on the effective melting point of the fuel and the requested margin with regards to detailed accident scenarios. However, precise calculations of the melting point of a U-MA dioxide are not available as of now. The pressure drop was computed using the Novendstern model for friction factor taken from [12] and the average power in the assembly was used. The mixing effects from the wrapper were not accounted for. The limiting value was taken as 134 kPa, which is the pressure drop for a regular fuel assembly.

2. Pre-design of the assembly

a. Thermomechanical behavior

A preliminary calculation was done using a standard fuel assembly design as given in Figure 1 and a fuel volume density equal to 43.67 %. Various geometrical designs, given in Table 2 , can be considered to achieve this density. As one can see here, the pressure drop is limited in the target assemblies due to their low power and large hydraulic diameters. The main dimensioning constraint is cladding resistance. For low diameter pin, a margin exists to increase the fuel centerline temperature.

Table 2 : Results for standard assembly designs

Number of rings	Pin diameter (mm)	Fuel centerline Temperature (°C)	Pressure drop (kPa)	Strain Criterion
8	10.59	1343	14.9	2.25
7	11.99	1488	11.8	2.55
6	13.83	1703	8.9	2.96

A preliminary optimization process based solely on pin diameter was carried out.. In this case, the gap, cladding and plenum dimensions are the ones reported in Figure 1. In order to accommodate the increase in gas production, the pin size must be decreased which limits the gases production but also the maximal achievable volume fraction. The best situation is obtained for minimal-size pin with a 5.8 mm diameter and 13 rings. The corresponding fuel volume fraction is 33 % with a pressure drop of 42 kPa. It was also observed that it was not possible to obtain a design with broader pins due to the necessity of respecting the strain criterion.

Several other options can be chosen to reduce the pin pressurization. The following were investigated here:

- Increase in the gap size in order to increase the pin free volume. This solution is limited by the fuel centerline temperature limit.
- Increase in the cladding size, which increases the pin resistance to pressurization.
- Increase in the plenum height up to 70 cm higher by extending the expansion volume into the sodium plenum. This solution increases the pressure drop but to a small extent.

When considering only pin diameter and plenum height, an optimum situation was found at a volume fraction of 41 % with 11 rings of 7.61 mm diameter, as shown on Figure 4. The limiting factor here is the cladding resistance due to pin pressurization. It was also not possible to obtain a design with fewer than 10 rings due to the strain criterion.

A last optimization process was carried out with regards to the four geometrical parameters, namely pin diameter, gap thickness, clad thickness and plenum height, the objective being to obtain the maximal fuel volume fraction in the target assembly in order to increase the transmutation performances in terms of mass consumption of minor actinides. Regarding those performances, it should be noted the relative efficiency of the transmutation process actually decreases when the fuel fraction increases due to spectral effects.

Looking at Figure 4, one can see that there is an optimum around 47 % for a 6 rings assembly. The competition between pin radius and pin pressurization explains this maximum. For low pin

diameters, the gas production is limited but the volume fraction is also limited as shown in Figure 2. On the other hand, big pin leads to increased fuel fraction but their diameter is restricted by the pin pressurization limit, which leads to a sub-optimal filling of the assembly. The optimum on Figure 4 corresponds to a situation with 169 pins of 14.33 mm of diameter with a gap thickness of 0.15 mm and a plenum height of 168.9 cm. The cladding thickness is 0.94 mm, or 85 % higher than for standard fuel assembly. This corresponds to a 47 % fuel volume fraction. Increasing the gap thickness does not prove to be an effective solution as it leads to a severe increase in fuel centerline temperature. The pressure drop for this optimized assembly design is 14 kPa, below the limiting value set at 134 kPa. The various data from each case are synthetized in Table 3.

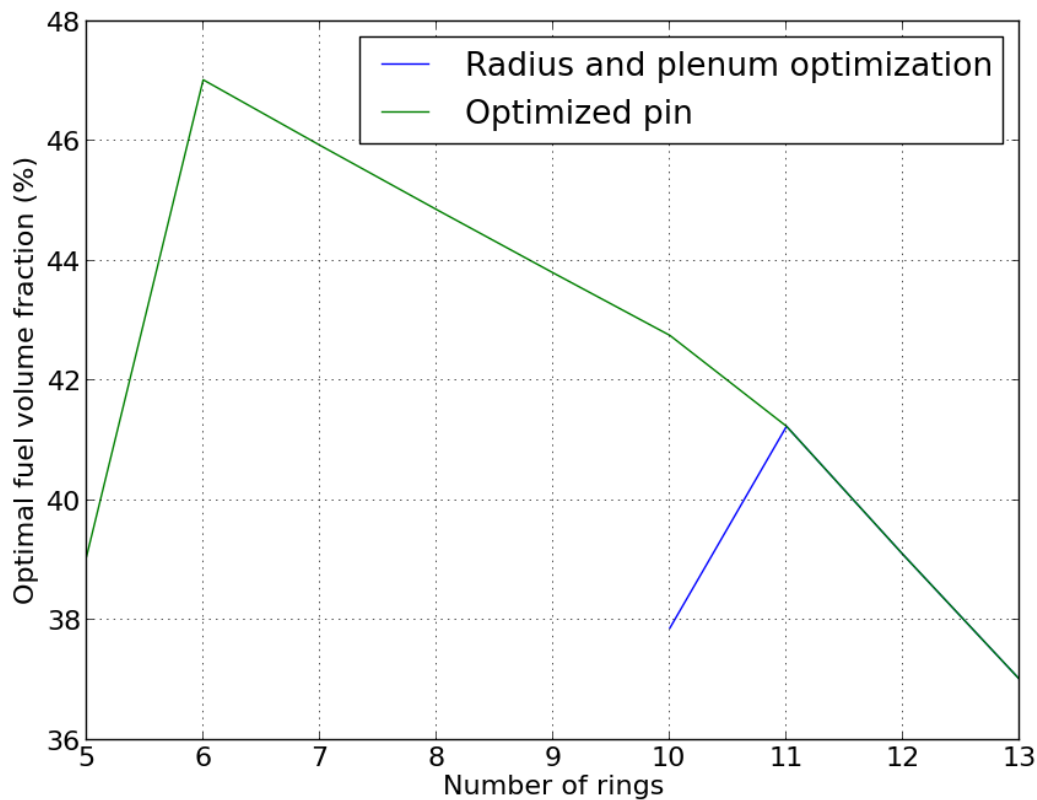


Figure 4: Optimal fuel volume fraction versus number of rings

We can see that it is possible to achieve a 12 points gain in absolute value in terms of fuel volume fraction, which translates both into an increase in the transmutation performances and a potential decrease in the assembly fabrication costs as fewer pins must be manufactured. The associated pressure drop is also smaller due to a larger hydraulic diameter in the assembly. The high linear power rate associated with big pins will also facilitate fuel restructuring and gas release, thus possibly validating *a posteriori* the total release hypothesis.

Table 3 : Comparison of the various assembly designs

	Radius optimization	Radius and plenum optimization	Optimized pin

Pin diameter (mm)	5.8	7.61	14.33
Number of rings	13	11	6
Cladding thickness (mm)	0.5	0.5	0.94
Gap thickness (mm)	0.15	0.15	0.15
Plenum height (mm)	98.9	168.9	168.9
Fuel volume fraction (%)	33	41	47

The sensitivity of the model to the constraints taken on fuel centerline temperature and on cladding strain was also evaluated, as shown in Figure 1. The fuel centerline constraint has a smaller impact than the strain constraint. This is explained by the fact that a lower maximal temperature requires a decrease in the pin radius while a lower acceptable constraint requires both a reduction of the pin radius and an increase in the cladding thickness.

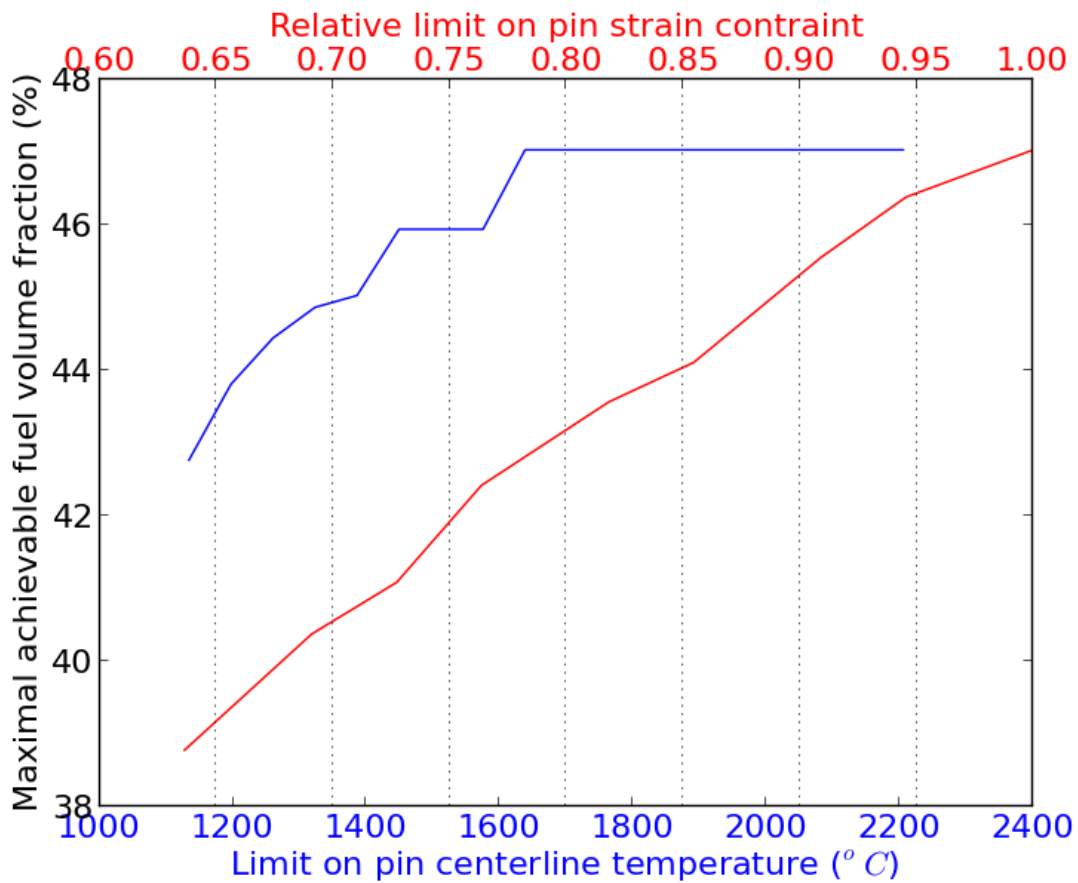


Figure 5 : Impacts of the constraints on the optimal fuel volume fraction

If we use the $1 \text{ W}\cdot\text{m}^{-1}\cdot\text{K}^{-1}$ minimal thermal conductivity as discussed before, the optimum case is slightly shifted towards smaller pins due to an increase in the fuel centerline temperature and an optimal fuel fraction of 43.5 % can be reached with 9 rings of pins with a diameter of 9.46 mm and a cladding thickness of 0.61 mm. The corresponding results are shown in

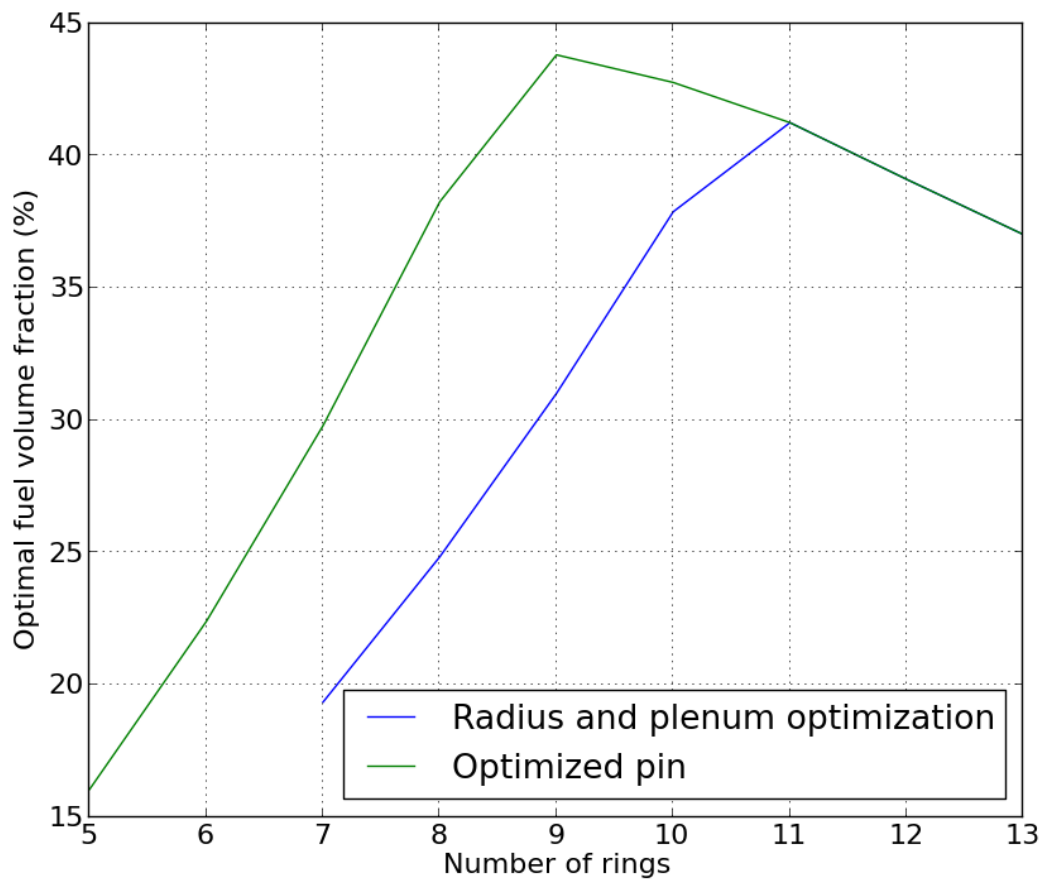


Figure 6 : Optimal fuel volume fraction versus number of rings for a fuel thermal conductivity of $1 \text{ W.m}^{-1}.\text{K}^{-1}$

b. Transmutation performances

In terms of transmutation performances, as one can see in Table 4, the increase in the fuel volume fraction leads to an amelioration of the transmutation performances by 33 % in terms of specific consumption. The efficiency of the process, expressed as the total transmutation rate, is two points lower in the optimized case due to spectral effects but this is compensated by the increase in the total mass loaded.

Table 4 : Comparison of the transmutation performances of the standard and optimized case

Standard case, fuel volume fraction = 33 %				
	Loaded mass (kg)	Unloaded mass (kg)	Transmutation rate (%)	Specific consumption (kg/Twhe)
Np	312	185	40,7	0,89
Am	1512	794	47,5	5,03

Cm	238	204	14,3	0,24
Total	2062	1183	42,6	6,16
Optimized case, fuel volume fraction = 47 %				
	Loaded mass (kg)	Unloaded mass (kg)	Transmutation rate (%)	Specific consumption (kg/Twhe)
Np	461	292	36,7	1,18
Am	2162	1204	44,3	6,71
Cm	314	268	14,6	0,32
Total	2937	1764	39,9	8,22

The impacts on the target assembly decay heat and neutron source were also assessed. When considering the heterogeneous transmutation strategy, it is necessary to take into account the added constraints on cooling time, transportation, reprocessing and manufacturing due to the high activity of the target assembly. The above-mentioned parameters were evaluated at 30 days and 5 years, which are times representative of the in-core handling and fuel transportation to the reprocessing plant. The results are given below in Table 5. However, considering Figure 4, one can see that tuning the fuel volume fraction in order to comply with fuel cycle constraints is achievable while keeping higher volume fraction than with the standard assembly design.

Table 5 : Impacts on assembly decay heat and neutron source

Standard case, fuel volume fraction = 33 %		
Decay heat (kw/assembly)	30 days	31,3
	5 years	7,5
Neutron source (1e8n/s/assembly)	30 days	0,57
	5 years	0,35
Optimized case, fuel volume fraction = 47 %		
Decay heat (kw/assembly)	30 days	41,4
	5 years	9,9
Neutron source (1e8n/s/assembly)	30 days	0,62
	5 years	0,4

3. Conclusion and perspectives

A pre-design of a target assembly for heterogeneous minor actinides transmutation in a SFR V2b core [13] was done using the hypothesis of complete gas release. Considering the set of assumptions used and a MABB cycle of 4100 EFPD, an optimum for the fuel volume fraction was found around 47 %, which corresponds to an hexagonal assembly with an increased plenum height and 12.31 mm of diameter pins with thicker cladding, +45 % compared to standard fuel pins used in the driver assemblies. The transmutation performances of the optimized assembly were computed along with the impacts on the fuel cycle and it was shown a corresponding 25 % increase in the consumption of minor actinides can be obtained. A continuation of this work will be done by using the GERMINAL code to extend the number of parameters taken into account and to validate the design. Other possible issues will also be investigated, such as swelling, fuel-cladding interaction or the important variation of power in the assembly during irradiation.

Bibliography

- [1] F. Varaine, L. Buiron, L. Boucher and D. Verrier, "Overview on homogeneous and heterogeneous transmutation in a new French SFR : reactor and fuel cycle impact," in *11th IEPMT*, San Francisco, 2010.
- [2] L. Buiron and e. al, "Heterogeneous minor actinides transmutation on a UO₂ blanket and on (U,Pu)O₂ fuel in sodium-cooled fast reactor. Assessment of core performances," in *GLOBAL*, Paris, 2009.
- [3] P.Sciora, L.Buiron, G.Rimpault and F.Varaine, "A break even oxide fuel core for an innovative French sodium-cooled fast reactor : neutronic studies results," in *GLOBAL*, Paris, 2009.
- [4] B.Valentin, H.Palancher, C.Yver, V.Garat and S.Massara, "Heterogeneous minor actinides transmutation on a UO₂ blanket and on (U,Pu)O₂ fuel in a Sodium Fast Reactor - Preliminary design of pin and sub-assembly," in *GLOBAL2009*, Paris, 2009.
- [5] G. Rimpault, "The ERANOS code and data system for fast reactor neutronic analyses," in *PHYSOR*, Seoul, 2002.
- [6] A. Tsilanizara, C. Diop, B. Nimal, M. Detoc*, L.Luneville, M. Chiron, T. Huynh, I. Bresard, M. Eid, J. Klein, B. Roque, P. Marimbeau, C. Garzenne, J. Parize and C. Vergne, "DARWIN: An Evolution Code System for a Large Range," *Journal of Nuclear Science and Technology*, vol. Supplement 1, pp. 845-849, 2000.
- [7] A. Santamarina, "The JEFF-3.1.1 Nuclear Data Library," OECD, Paris, 2009.
- [8] A. Waltar and A. Reynolds, "Chapter 8 : Fuel pin and assembly design," in *Fast Breeder Reactors*, New York, Pergamon Press, 1981, pp. 251-312.
- [9] N. T., I. A., Ichise.K and A. Y., "Heat capacities and thermal measurements of AmO₂ et AmO_{1.5}," in *NuMat*, Karlsruhe, 2010.
- [10] E. Bich, J. Millat and E. Vogel, "The viscosity and thermal conductivity of pure monatomic gases from their normal boiling point up to 5000 K in the limit of zero density and at 0.101325 MPa," *Phys. Chem. Ref. Data*, vol. 9, no. 19, p. 128, 1990.
- [11] R. J. M. Koning, L. R. Morss and J. Fuger, "Thermodynamic Properties of Actinides and Actinide Compounds," in *The chemistry of the actinide and transactinides elements*, The Netherlands, Springer, 2011, p. 2135.
- [12] A. Waltar and A. Reynolds, "Chapter 10 : Core thermal hydraulics design," in *Fast Breeder Reactors*, New York, Pergamon Press, 1981, pp. 376-377.
- [13] P. Sciora, D. Blanchet, L. Buiron, B. Fontaine, M. Vanier, F. Varaine, C. Venard, S. Massara, A.

Scholar and D. Verrier, "Low void effect core design applied on 2400 MWth SFR reactor," in *ICAPP 2011*, Nice, France, 2011.

- [14] G. N. C.T Walker, "Transmutation of neptunium and americium in a fast neutron flux: EPMA results and KORIGEN predictions for the superfact fuels," *Journal of Nuclear Materials*, vol. 218, no. 2, pp. 129-138, 1995.